Title	Element-specific observation of the ferromagnetic ordering process in UCoAl via soft X-ray magnetic circular dichroism
Author(s)	Takeda Yukiharu, Saito Yuji, Okane Tetsuo, Yamagami Hiroshi, Matsuda Tatsuma, Yamamoto Etsuji, Haga Yoshinori, Onuki Yoshichika
Citation	Physical Review B,97(18),p.184414_1-184414_7
Text Version	Version of Record
URL	https://jopss.jaea.go.jp/search/servlet/search?5063581
DOI	https://doi.org/10.1103/PhysRevB.97.184414
Right	© American Physical Society

Element-specific observation of the ferromagnetic ordering process in UCoAl via soft x-ray magnetic circular dichroism

Yukiharu Takeda,* Yuji Saitoh, and Tetsuo Okane
Materials Sciences Research Center, Japan Atomic Energy Agency, 1-1-1 Kouto, Sayo-cho, Sayo-gun, Hyogo 679-5148, Japan

Hiroshi Yamagami
Materials Sciences Research Center, Japan Atomic Energy Agency, 1-1-1 Kouto, Sayo-cho, Sayo-gun, Hyogo 679-5148, Japan and Department of Physics, Kyoto Sangyo University, Motoyama, Kamigamo, Kita-Ku, Kyoto 603-8555, Japan

Tatsuma D. Matsuda
Department of Physics, Tokyo Metropolitan University, 1-1 Minami-Osawa, Hachioji-shi, Tokyo 192-0397, Japan

Etsuji Yamamoto and Yoshinori Haga
Advanced Science Research Center, Japan Atomic Energy Agency, Tokai, Ibaraki 319-1195, Japan

Yoshichika Ōnuki
Department of Physics and Earth Sciences, Faculty of Science, University of the Ryukyus, Nishihara, Okinawa 903-0213, Japan

(Received 24 March 2017; revised manuscript received 1 February 2018; published 10 May 2018; corrected 13 June 2018)

We have performed soft x-ray magnetic circular dichroism (XMCD) experiments on the itinerant-electron metamagnet UCoAl at the U $4d-5f(N_{4,5})$ and Co $2p-3d(L_{2,3})$ absorption edges in order to investigate the magnetic properties of the U $5f$ and Co $3d$ electrons separately. From the line shape of the XMCD spectrum, it is deduced that the orbital magnetic moment of the Co $3d$ electrons is unusually large. Through the systematic temperature (T)- and magnetic field (H)-dependent XMCD measurements, we have obtained two types of the magnetization curve as a function of H and T (M-H curve and M-T curve, respectively). The metamagnetic transition from a paramagnetic state to a field-induced ferromagnetic state was clearly observed under 15 K at H_M. The value of the H_M and its T dependence agree well between the U and Co sites, and the bulk magnetization. Whereas, we have discovered the remarkable differences in the M-H and M-T curves between the U and Co sites. The present findings clearly show that the role of the Co $3d$ electrons should be considered more carefully in order to understand the origin of the magnetic ordering in UCoAl.

DOI: 10.1103/PhysRevB.97.184414

I. INTRODUCTION

The occurrence of ferromagnetic (FM) ordering in uranium compounds is very attractive in condensed-matter physics because uranium compounds, such as UGe_2 [1], URhGe [2], and UCoGe [3], display a coexistence of superconductivity and ferromagnetism. Although magnetism in uranium compounds has been studied from both theoretical and experimental sides, unsolved issues about the origin of the magnetic ordering have remained due to difficulties to grasp the nature of the U $5f$ electrons, namely, the duality of itinerant and localized, and to understand complicated interactions between the U $5f$ and other electrons.

The uranium ternary compound UCoAl crystallizes in the ZrNiAl-type hexagonal structure [4]. When the magnetic field (H) is applied along the c axis, the metamagnetic transition (MMT) from a paramagnetic (PM) state to a field-induced FM state occurs at the critical magnetic field H_M in the low-temperature (T) region. The MMT is strongly anisotropic between $H \parallel$ and $\perp$ c axis, indicating an Ising-like magnetic behavior [5–7]. Since the ground state of UCoAl is the PM state, it is considered that UCoAl is classified as an itinerant metamagnet. As T goes up, the first-order MMT changes to a crossover at the critical end point (CEP), (T_0, H_0) = ($\sim$10–12 K, $\sim$0.8–1.0 T), determined by the magnetization [8,9], the ac susceptibility [9], the magnetoresistance [10], the nuclear magnetic resonance (NMR) [11,12], the thermoelectric power [13], and the Hall effect [14]. Compared to classical itinerant metamagnets such as YCo_2 and $LuCo_2$, the H_M in UCoAl is much lower than that in these compounds ($H_M \sim 70$ T) [15,16], which makes it easier to investigate the magnetic ordering process by various experiments.

The T dependence of the magnetic moment (M-T curve) in UCoAl shows a peak around 20 K [8]. As T decreases and H increases, the peak in the M-T curve seems to link continuously with the field-induced FM state. The NMR measurements using ^{59}Co and ^{27}Al nuclei [11,12] have revealed that the peak in the M-T curve is ascribed to the longitudinal spin

*ytakeda@spring8.or.jp

fluctuation along the c axis. It is considered here that the spin-fluctuation behavior should be derived dominantly from the U $5f$ electrons as a plausible interpretation. However, the magnetic stability of UCoAl is very sensitive to the elemental substitution for Co and Al atoms [17–21]. For example, in the case of the $UCo_{1-x}Ru_xAl$ system [19,21], the ferromagnetism already appears for very low Ru content with $x = 0.01$ and persists up to $x \sim 0.75$, although both of the parent compounds, UCoAl and URuAl, are in a PM ground state. It implies that the magnetic stability is strongly affected by the interactions between the U $5f$ and Co $3d$ electrons. Therefore, element-specific investigations of magnetic properties changing T and H provide us with crucial information about the FM ordering process. In principle, x-ray magnetic circular dichroism (XMCD) is a powerful magnetic probe with element- and electronic-shell-specific characteristics because the core absorption process is utilized. Using the U $N_{4,5}$ $(4d - 5f)$ and Co $L_{2,3}(2p - 3d)$ absorption edges, which coexist in the soft x-ray region, the magnetic properties of the U $5f$ and Co $3d$ electrons can be extracted separately [22]. Since, unfortunately, the photon-energy regions at the U N_4 and Co L_3 edges overlap each other, it is difficult to estimate the spin and orbital magnetic moments quantitatively using the XMCD sum rules [23,24]. Meanwhile, the element-specific magnetization curve (M-H curve) measurements can be done by taking the H dependence of the XMCD intensity at the U N_5 and Co L_2 edges, as reported in the previous XMCD study [25]. In this paper, we promote the systematic T- and H-dependent XMCD study to grasp the magnetic ordering process from the PM to the field-induced FM states in UCoAl. The present findings suggest that the magnetic properties of the Co $3d$ electrons play an important role in the FM ordering process in UCoAl.

II. EXPERIMENT

We used single crystals grown by the Czochralski method in a tetra-arc furnace. The detailed procedure of the sample growth is presented in Ref. [8]. The residual resistivity ratio is approximately 27, indicating that the quality of the sample is very good among the samples used in other experiments so far. The XMCD experiments at the U $N_{4,5}$ and the Co $L_{2,3}$ edges were carried out at the beam line BL23SU of SPring-8. A clean surface of the sample was prepared by fracturing in ultrahigh vacuum. The T of the sample was controlled between 5.6 and 50 K using a liquid-helium cryostat. The external H up to 7 T was applied along the c axis, the easy axis of magnetization, using a superconducting magnet. The incident circularly polarized x ray irradiated the sample along the direction of magnetization. X-ray absorption spectra (XAS) were measured by the total electron yield method. In the beam line, the photon helicity can be switched at 1 Hz using a combination between a pair of twin-helical undulators of in-vacuum type and five kicker magnets [26]. The XMCD signals were collected by switching the photon helicity at each energy point. The XMCD data displayed in this paper were averaged by reversing the H direction in order to remove the artificial effects such as an inevitable asymmetry of the XMCD measurement system.

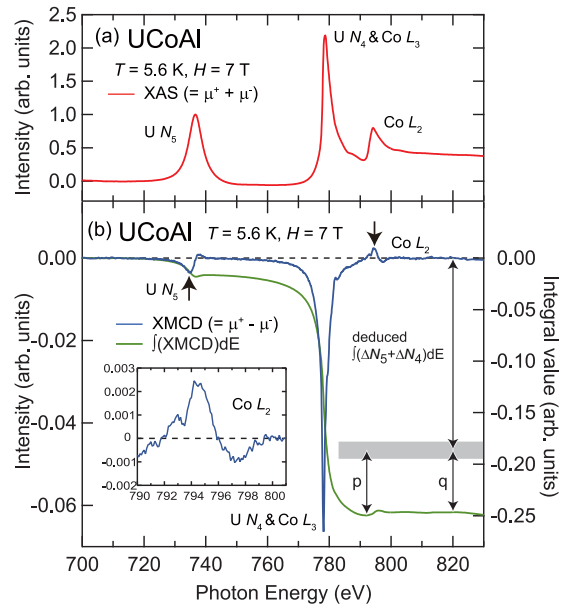

FIG. 1. Experimental (a) XAS and (b) XMCD spectra at the U $N_{4,5}$ and Co $L_{2,3}$ absorption edges recorded at $T = 5.6$ K and $H = 7$ T. In (b), the integral of the XMCD spectrum is plotted together. The gray hatched bar shows an integral value for the U $N_{4,5}$ edges estimated using the XMCD spectra at the U $M_{4,5}$ edge [28,29]. The error of the estimation is expressed by the width of the gray bar. Based on the estimation of the integral value for the U $N_{4,5}$ edges, the p and q values can be regarded as integral values for the Co L_3 and $L_{2,3}$ edges, respectively. The up and down arrows show the main peaks at the U N_5 ($h\nu = 735.9$ eV) and Co L_2 ($h\nu = 794.5$ eV) edges, respectively. The inset shows an enlarged figure around the Co L_2 edge.

III. RESULTS AND DISCUSSION

Figures 1(a) and 1(b) show the XAS and XMCD spectra of UCoAl at the U $N_{4,5}$ and Co $L_{2,3}$ edges. The spectra were obtained in the field-induced FM state at $T = 5.6$ K and $H = 7$ T. Here, μ^+ (μ^-) refers to the x-ray absorption coefficient for the photon helicity parallel (antiparallel) to the magnetization direction. The intensity of the XMCD spectrum defined as $(\mu^+ - \mu^-)$ is normalized so that the intensity of XAS $(\mu^+ + \mu^-)$ from the pre-edge ($h\nu = 720$ eV) to the peak top at the U N_5 edge ($h\nu = 736.6$ eV) becomes unity. Although the two pairs of the spin-orbit splitting exist in the photon-energy region, namely, corresponding to the U $N_{4,5}$ and Co $L_{2,3}$ edges, three peaks are observed mainly in the XAS and the XMCD spectrum due to the overlap of the Co L_3 and U N_4 edges around $h\nu = 778$ eV [27].

In Fig. 1(b), the integral of the XMCD spectrum is also plotted (green line). In principle, the information about the U $5f$ electrons obtained from the XMCD spectra at the U $N_{4,5}$ edges should be identical to that at the U $M_{4,5}$ edges. Two XMCD experiments at the U $M_{4,5}$ edges have been reported so far [28,29]. We have deduced the integral value of the XMCD spectrum at the U $N_{4,5}$ edges so that it satisfies the intensity ratio of the XMCD spectra at the U $M_{4,5}$ edges. By subtracting the integral value at the U $N_{4,5}$ edges from the total integral value at the U $N_{4,5}$ and Co $L_{2,3}$ edges, the integral values for the Co L_3 (p) and $L_{2,3}$ (q) edges can be

obtained, as indicated by double-headed arrows [30]. Note that the contribution at the Co L_2 edge to the integral value q becomes small because the XMCD spectrum at the Co L_2 edge consists of the positive and negative peaks, which partially cancel each other, as shown in the inset of Fig. 1(b). This leads to a large residual q value [31]. According to the sum rules for the $L_{2,3}$ edges [23,24], the ratio $\delta = \langle L_Z\rangle/(2\langle S_Z\rangle + 7\langle T_Z\rangle)$ can be expressed as $\delta = 2q/(9p - 6q)$, which is independent of the occupation number of the Co $3d$ electrons and the intensity of the XAS spectrum. Here, $\langle L_Z\rangle$, $\langle S_Z\rangle$, and $\langle T_Z\rangle$ are the expectation values of the z component of the orbital angular momentum, the spin angular momentum, and the magnetic dipole operator, respectively. The orbital magnetic moment and the spin magnetic moment are described as $M_L = -\langle L_Z\rangle\mu_B$ and $M_S = -2\langle S_Z\rangle\mu_B$, respectively. Surprisingly, the value of δ reaches ~0.5–0.6, which is much larger than that of Co metal with $\delta = 0.095$ [32]. The large value of δ suggests that the M_L is enhanced significantly and the spatial distribution of the Co $3d$ electrons is strongly distorted, which might be caused through the U($5f$)-Co($3d$) hybridization. Moreover, one can notice similarity about the enhancement of the M_L in the case of URhGe. The XMCD experiment at the Rh $L_{2,3}$ edges has revealed that the value of δ is 0.67 for the Rh $4d$ electrons because no XMCD signal is detected at the Rh L_2 edge [33]. The enhancement of δ of the Co $3d$ electrons in UCoAl seems to be somewhat smaller than that of the Rh $4d$ electrons in URhGe. It could be interpreted that the hybridization between the U $5f$ and the Co $3d$ electrons in UCoAl is weaker than that between the U $5f$ and the Rh $4d$ electrons in URhGe, as discussed in the polarized neutron diffraction (PND) study [4]. It implies that the enhancement of δ on the transition elements is a significant phenomenon to understand how the interaction between the U $5f$ electrons and other ones plays in U-based compounds.

By collecting the H dependence of the XMCD intensity at the U N_5 ($h\nu = 735.0$ eV) and Co L_2 ($h\nu = 794.5$ eV) edges, indicated by arrows in Fig. 1(b), we obtained the element-specific M-H curves at the U and Co sites, as shown in Figs. 2(a) and 2(b), respectively. The M-H curves measured at the selected T between 5.6 and 50 K. All the M-H curves are normalized so that the XMCD intensity becomes unity at $T = 5.6$ K and $H = 7$ T. At low Ts, the MMT is clearly observed as a steep jump of the XMCD intensity. Then the MMT gradually smears out as T increases [34]. The values of the H_M are determined by the second derivative of each M-H curve. Using this method, the values of H_M were able to be estimated under 15 K from the element-specific M-H curves. Figure 3 shows the T dependence of the H_M at each site, indicating that there is no difference between the U and Co sites. In addition, the T dependence of the element-specific H_M agrees well with the result obtained by the bulk magnetization measurement [8]. This clearly indicates that the intrinsic magnetic properties are extracted by the present XMCD experiment.

According to the high-field magnetization measurement [35], the magnetic moment continues to increase almost linearly with H even in the field-induced FM state and does not saturate even above H_M up to 39 T. The XMCD intensities at both sites are also increased as H increases [Figs. 2(a) and 2(b)]. Figure 4 shows the slope of the M-H curve in the high-H region (S_{high}) as a function of T. In order to extract

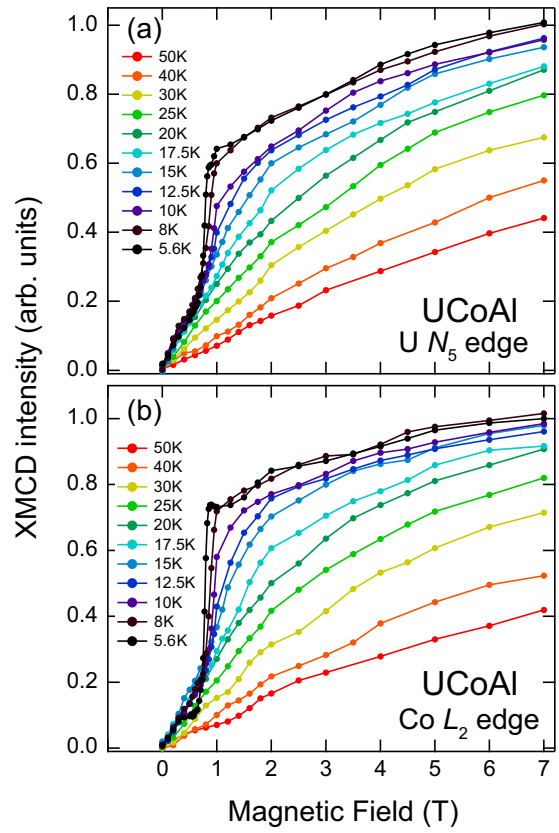

FIG. 2. H dependence of the XMCD intensity (M-H curve) at several Ts. (a) The M-H curve at the U N_5 edge ($h\nu = 735.0$ eV) and (b) that at the Co L_2 edge ($h\nu = 794.5$ eV). These photon-energy positions are indicated by the arrows, as shown in Fig. 1(b). The M-H curves are normalized so that the XMCD intensity at $T = 5.6$ K and $H = 7$ T becomes 1.

the S_{high}, we have fitted each M-H curve for $H > 3$ T with a straight line (see an example in the inset of Fig. 4), namely, $S_{high} = \Delta\text{XMCD}/\Delta H_{H>3T}$. The scale of the vertical axis in Fig. 4 is the same as that in Figs. 2(a) and 2(b). The values of the S_{high} at the U and Co sites are almost the same between 30 and 50 K, and increase similarly as T decreases. With further

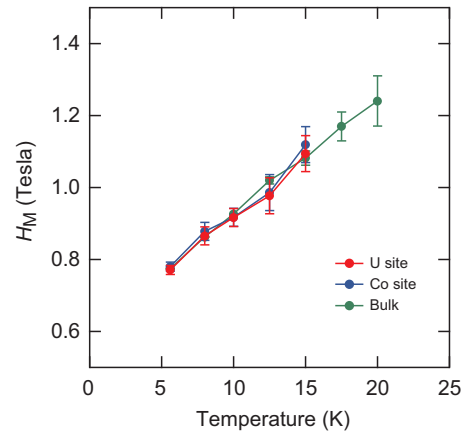

FIG. 3. T dependence of the H_M determined by the second derivative of each M-H curve. Above 17.5 K, the M-H curves are too broad to estimate the H_M.

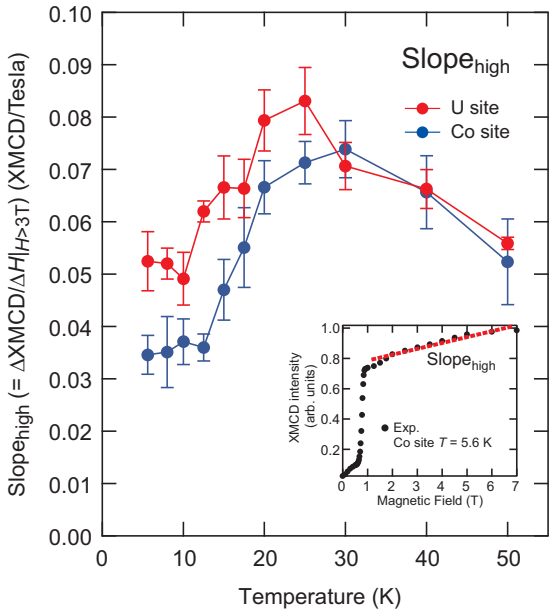

FIG. 4. T dependence of the slope of the element-specific M-H curve in the high magnetic field region (S_{high}), obtained by fitting the M-H curve above $H = 3$ T with a straight line. The scale of the vertical axis is the same as that in Figs. 2(a) and 2(b). The inset shows an example of the S_{high} at the Co site at 5.6 K.

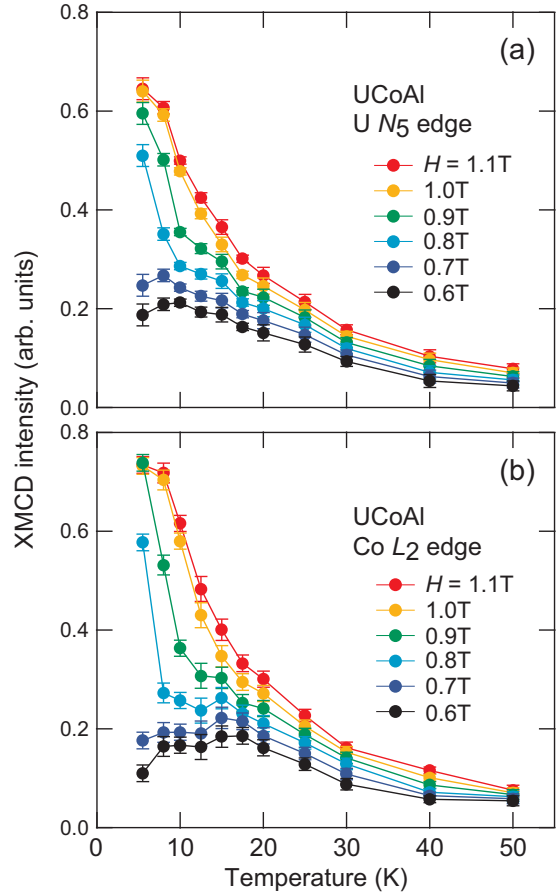

FIG. 5. T dependence of the XMCD intensity (M-T curve) between $T = 5.6$ and 50 K. The M-T curves under $H = 0.6$, 0.7, 0.8, 0.9, 1.0, 1.1 T at the (a) U and (b) Co sites.

cooling, a broad peak is observed between 20 and 30 K as a common feature in the S_{high}. Below 10 K ($\sim T_0$), where the MMT clearly appears, the S_{high} seems to be independent of T. In order to compare the T dependence of the S_{high} between both sites, we have normalized the S_{high} at 5.6 K (lowest T) and 25 K (around the peak) using the value of the S_{high} at 50 K (highest T) for each site. As for the U site, the ratios S_{high}(5.6 K)/S_{high}(50 K) and S_{high}(25 K)/S_{high}(50 K) are of the order of 0.93 and 1.48, respectively. As for the Co site, they are 0.66 and 1.36. The value of the S_{high}(25 K)/S_{high}(50 K) at the Co site is comparable to that at the U site within errors. The magnetic response at the Co site seems to be similar to that at the U site between $T = 50$ K and $\sim$25 K. On the other hand, the S_{high}(5.6 K)/S_{high}(50 K) at the Co site becomes smaller than that at the U site, meaning that the M-H curves are bent toward the H axis more strongly at the Co site than at the U site, especially below T_0. Indeed, the PND experiments have revealed the different H dependence of the magnetic moments between the U and Co sites in the induced FM states at low Ts [4,36].

Next, in order to investigate the T dependence of the XMCD intensity around H_M, we reconstruct element-specific M-T curves by swapping the H and T axes in Figs. 2(a) and 2(b). Figures 5(a) and 5(b) show the M-T curves from 0.6 to 1.1 T at the U and Co sites, respectively. As H increases and T decreases, the XMCD intensity at each site gradually increases. The appearance of the MMT is clearly seen around T_0 and H_M, for example, the M-T curves taken at 0.8 and 0.9 T, which is consistent with the bulk magnetization measurement [8]. Figures 6(a) and 6(b) show the M-T curves taken at 1.1 and 0.7 T, respectively, and the M-T curves by the bulk magnetization taken at the same H are plotted together. The profiles in Figs. 6(a) and 6(b) are normalized so that the value at 5.6 K becomes unity. At 1.1 T just above H_M, the XMCD intensities at both sites increase as T decreases. The profiles of the M-T curves above H_M are very similar and agree well with that of the bulk magnetization, as shown in Fig. 6(a). The agreement between the element-specific and bulk profiles suggests that the bulk magnetic property is explained well by the U 5f and Co 3d electrons above H_M. On the other hand, at 0.7 T just below H_M, the element-specific M-T curves at both sites seem to deviate from the bulk M-T curve, unlike above H_M. The deviation in the M-T curve implies that other conduction electrons, except for the U 5f and Co 3d electrons, contribute considerably to the bulk magnetic property. Indeed, we have confirmed that the magnetic polarization at the nonmagnetic Al site obviously exists, as described in the Appendix. Meanwhile, as shown in Fig. 6(c), the inverse plots of the M-T curves taken at 0.7 T converge on one straight line above 25 K, indicating that they obey the Curie-Weiss law. Accordingly, the Weiss temperatures for the bulk, i.e., the U and Co sites are almost the same value which is estimated as 13.1 ± 0.5 K, are very close to the value of T_0 ($\sim$10–12 K).

Comparing the M-T curves between the U and Co sites, as shown in Fig. 6(b), we emphasize that the peak in the M-T curve at the Co site develops more strongly than that at the U site between 15 and 20 K (indicated by a black arrow). According to the NMR experiments [11,12], it is

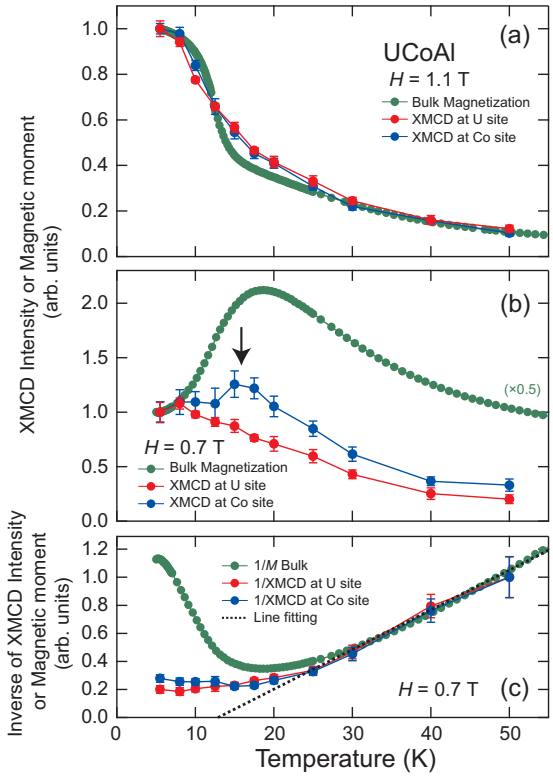

FIG. 6. Comparison between the element-specific and bulk M-T curves [8]. (a) At $H = 1.1$ T above H_M. (b) At $H = 0.7$ T below H_M. The profiles in (a) and (b) are normalized at $T = 5.6$ K. The M-T curve of the bulk magnetization at $H = 0.7$ T is multiplied by 0.5. (c) Inverse plots of the M-T curves at $H = 0.7$ T displayed in (b), which is normalized at $T = 50$ K for easy comparison.

interpreted that the peak in the bulk M-T curve is ascribed to the spin-fluctuation behavior along the c axis. Therefore, the origin of the peak in the element-specific M-T curves connects naturally to the spin-fluctuation behavior, meaning that the magnetic properties not only at the U site but also at the Co site play an important role in the spin-fluctuation behavior. In addition, there is the clear difference in the T dependence of S_{high} between the U and Co sites, especially below T_0, as shown in Fig. 4. The large value of δ of the Co $3d$ electrons, as shown in Fig. 1(b), suggests the Co $3d$ electrons possess the particular electronic states, which could be a clue to understand how the U $5f$ and the Co $3d$ electrons hybridize each other. Therefore, we consider that the role of the Co $3d$ electrons should be considered more carefully in order to understand the origin of the magnetic ordering in UCoAl. We hope that the present findings stimulate both theoretical and experimental research for the element- and shell-dependent magnetic properties in uranium compounds.

IV. SUMMARY

We have investigated the local magnetic properties in UCoAl using the soft x-ray XMCD at the U $N_{4,5}$ and Co $L_{2,3}$ absorption edges. Applying the sum rules to the XMCD spectrum, it is found that the M_L of the Co $3d$ electrons is significantly increased. From the systematic T- and H-dependent XMCD study, we have succeeded in extracting the element-specific magnetic properties of the U $5f$ and Co $3d$ electrons and have observed the FM ordering process microscopically associated with the MMT in UCoAl. The MMT is clearly observed at both the U and Co sites below 15 K at H_M. The T dependence of H_M observed by the XMCD experiments agrees well with that obtained by the bulk magnetization measurement. Meanwhile, we have revealed that there are noticeable differences in the magnetic properties between the U and Co sites. Although the S_{high} shows the similar T dependence at the U and Co sites above $T \sim 25$ K, the S_{high} is decreased more remarkably at the Co site than at the U site, especially below $T = 10$ K. The peak in the M-T curve at $H = 0.7$ T, which could be related to the spin-fluctuation behavior, is developed around $T \sim 20$ K at the Co site more strongly than at the U site. The present results indicate that the magnetic properties of the Co $3d$ electrons cannot be explained only by that of the U $5f$ electrons. Therefore, we consider that the role of the Co $3d$ electrons should be considered more carefully in order to understand the origin of the MMT in UCoAl. We have demonstrated that the systematic T- and H-dependent XMCD experiments provide valuable information about the magnetic ordering process in materials composed of plural magnetic elements.

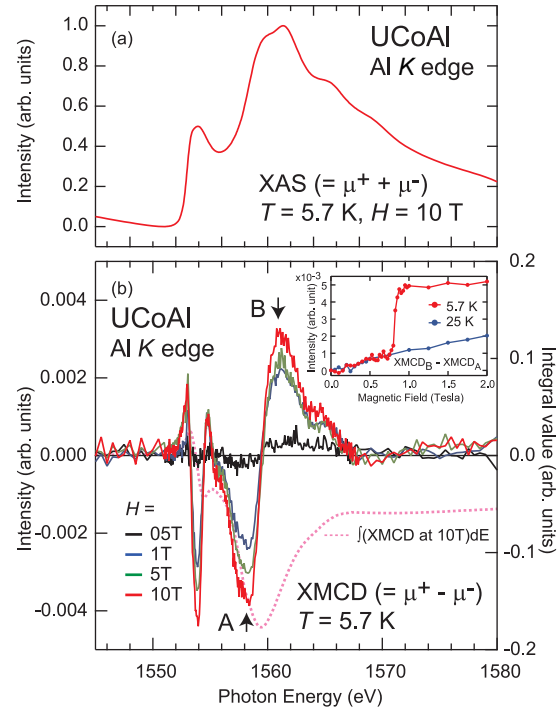

FIG. 7. XAS and XMCD spectra at the Al K absorption edge. (a) XAS spectrum taken at $T = 5.7$ K and $H = 10$ T. (b) XMCD spectra taken at $H = 0.5$, 1, 5, and 10 T. The integral of the XMCD spectrum taken at $H = 10$ T is plotted together (pink dashed line). The inset shows the element-specific M-H curve at the Al site, obtained by the amplitude between the XMCD signals recorded at $h\nu = 1558.3$ (arrow A) and 1561.3 eV (arrow B). The M-H curves taken at $T = 5.7$ and 25 K are displayed.

ACKNOWLEDGMENTS

The authors would like to thank Z. Fisk for valuable discussions and S-i. Fujimori for great support regarding the experimental preparation of uranium compounds. The experiments were performed under Proposals No. 2011B3825, No. 2014A3821, No. 2014B3821, No. 2015A3820, No. 2015B3820, and No. 2017A3811 of SPring-8 BL23SU. This work was financially supported by a Grant-in-Aid for Scientific Research on Innovative Areas "Heavy Electrons" (Grant No. 20102003) from the Ministry of Education, Culture, Sports, Science and Technology (MEXT) Japan, and by Grant-in-Aid for Young Scientists (B) No. 25800207 from Japan Society for the Promotion of Science (JSPS).

APPENDIX: XAS AND XMCD AT THE AL *K* ABSORPTION EDGE OF UCOAL

Figure 7(a) shows the XAS spectrum at the Al K edge of UCoAl taken at $T = 5.7$ K and $H = 10$ T, which is normalized so that the XAS intensity at $h\nu = 1561.3$ eV becomes unity. We have confirmed that the shape of the XAS spectrum at $T = 5.7$ K is not changed with H. Note that we have detected obvious XMCD signals even at the nonmagnetic Al site, as shown in Fig. 7(b), indicating that the magnetic polarization of the Al $3p$ electrons exists. The XMCD intensity depends on the strength of H, but the shape of the XMCD spectra is not changed. The integral of the XMCD spectrum at $H = 10$ T from $h\nu = 1545$ eV up to 1580 eV results in a negative value (pink dashed line). According to the sum rules [23,24] for the K edge, the negative value leads to a conclusion that the Al $3p$ electrons have a finite orbital magnetic moment and it turns to the H direction i.e., parallel to the direction of the total magnetic moments at the U and Co sites.

In order to obtain the element-specific M-H curve at the Al site, we have recorded the H dependence of the XMCD signals at $h\nu = 1558.3$ and 1561.3 eV (denoted by arrows A and B, respectively). The inset of Fig. 7(b) plots the H dependence of the amplitude between the negative (A) and positive (B) XMCD peaks (i.e., $\mathrm{XMCD_B} - \mathrm{XMCD_A}$) for a good signal-to-noise ratio. The M-H curve taken at $T = 25$ K is displayed together. At $T = 25$ K, the M-H curve shows the PM behavior. On the other hand, the MMT is clearly observed at $T = 5.7$ K, and the value of H_M at the Al site is the same as the U and Co sites (Fig. 3). The result indicates that the magnetic polarization at the Al site contributes to the magnetism of this compound. Indeed, the existence of the magnetic polarization at the Al site and its orientation are consistent with the results of the PND experiment [4]. In the PND experiment, they have reported that the magnetic moment at the Al site is comparable to that at the Co site. However, we cannot estimate the magnitude of the magnetic moments quantitatively and cannot compare the values of the magnetic moments at each site in the present study.

[1] S. S. Saxena, P. Agarwal, K. Ahilan, F. M. Grosche, R. K. W. Haselwimmer, M. J. Steiner, E. Pugh, I. R. Walker, S. R. Julian, P. Monthoux, G. G. Lonzarich, A. Huxley, I. Sheikin, D. Braithwaite, and J. Flouquet, Nature (London) **406**, 587 (2000).

[2] D. Aoki, A. Huxley, E. Ressouche, D. Braithwaite, J. Flouquet, J.-P. Brison, E. Lhotel, and C. Paulsen, Nature (London) **413**, 613 (2001).

[3] N. T. Huy, A. Gasparini, D. E. de Nijs, Y. Huang, J. C. P. Klaasse, T. Gortenmulder, A. de Visser, A. Hamann, T. Görlach, and H. v. Löhneysen, Phys. Rev. Lett. **99**, 067006 (2007).

[4] P. Javorský, V. Sechovský, J. Schweizer, F. Bourdarot, E. Lelièvre-Berna, A. V. Andreev, and Y. Shiokawa, Phys. Rev. B **63**, 064423 (2001).

[5] T. D. Matsuda, Y. Aoki, H. Sugawara, H. Sato, A. V. Andreev, and V. Sechovsky, J. Phys. Soc. Jpn. **68**, 3922 (1999).

[6] T. D. Matsuda, H. Sugawara, Y. Aoki, H. Sato, A. V. Andreev, Y. Shiokawa, V. Sechovsky, and L. Havela, Phys. Rev. B **62**, 13852 (2000).

[7] N. V. Mushnikov, T. Goto, K. Kamishima, H. Yamada, A. V. Andreev, Y. Shiokawa, A. Iwao, and V. Sechovsky, Phys. Rev. B **59**, 6877 (1999).

[8] T. D. Matsuda, N. Tateiwa, E. Yamamoto, Y. Haga, Y. Ōnuki, D. Aoki, J. Flouquet, and Z. Fisk, J. Korean Phys. Soc. **63**, 575 (2013).

[9] N. Kimura, N. Kabeya, H. Aoki, K. Ohyama, M. Maeda, H. Fujii, M. Kogure, T. Asai, T. Komatsubara, T. Yamamura, and I. Satoh, Phys. Rev. B **92**, 035106 (2015).

[10] D. Aoki, T. Combier, V. Taufour, T. D. Matsuda, G. Knebel, H. Kotegawa, and J. Flouquet, J. Phys. Soc. Jpn. **80**, 094711 (2011).

[11] K. Karube, T. Hattori, S. Kitagawa, K. Ishida, N. Kimura, and T. Komatsubara, Phys. Rev. B **86**, 024428 (2012).

[12] H. Nohara, H. Kotegawa, H. Tou, T. D. Matsuda, E. Yamamoto, Y. Haga, Z. Fisk, Y. Ōnuki, D. Aoki, and J. Flouquet, J. Phys. Soc. Jpn. **80**, 093707 (2011).

[13] A. Palacio-Morales, A. Pourret, G. Knebel, T. Combier, D. Aoki, H. Harima, and J. Flouquet, Phys. Rev. Lett. **110**, 116404 (2013).

[14] T. Combier, D. Aoki, G. Knebel, and J. Flouquet, J. Phys. Soc. Jpn. **82**, 104705 (2013).

[15] T. Goto, T. Sakakibara, K. Murata, H. Komatsu, and K. Fukamichi, J. Magn. Magn. Mater. **90-91**, 700 (1990).

[16] T. Goto, H. A. Katori, T. Sakakibara, H. Mitamura, K. Fukamichi, and K. Murata, J. Appl. Phys. **76**, 6682 (1994).

[17] A. Andreev, V. Sechovský, N. Mushnikov, T. Goto, Y. Homma, and Y. Shiokawa, J. Alloys Compd. **306**, 72 (2000).

[18] A. Andreev, A. Chernyavsky, N. Izmaylov, and V. Sechovsky, J. Alloys Compd. **349**, 12 (2003).

[19] A. V. Andreev, L. Havela, V. Sechovsk, M. I. Bartashevich, J. Šebek, R. V. Dremov, and I. K. Kozlovskaya, Philos. Mag. B **75**, 827 (1997).

[20] A. Andreev, K. Shirasaki, J. Šebek, J. Vejpravov, D. Gorbunov, L. Havela, S. Daniš, and T. Yamamura, J. Alloys Compd. **681**, 275 (2016).

[21] J. Pospíšil, P. Opletal, M. Vališka, Y. Tokunaga, A. Stunault, Y. Haga, N. Tateiwa, B. Gillon, F. Honda, T. Yamamura, V. Nižňanský, E. Yamamoto, and D. Aoki, J. Phys. Soc. Jpn. **85**, 034710 (2016).

[22] UCoAl with the ZrNiAl-type hexagonal structure has two different sites for Co atoms. The magnetic properties between

the two Co sites cannot be distinguished in the present XMCD experiment.

[23] B. T. Thole, P. Carra, F. Sette, and G. van der Laan, Phys. Rev. Lett. **68**, 1943 (1992).

[24] P. Carra, B. T. Thole, M. Altarelli, and X. Wang, Phys. Rev. Lett. **70**, 694 (1993).

[25] Y. Takeda, Y. Saitoh, T. Okane, H. Yamagami, T. D. Matsuda, E. Yamamoto, Y. Haga, Y. Ōnuki, and Z. Fisk, Phys. Rev. B **88**, 075108 (2013).

[26] Y. Saitoh, Y. Fukuda, Y. Takeda, H. Yamagami, S. Takahashi, Y. Asano, T. Hara, K. Shirasawa, M. Takeuchi, T. Tanaka, and H. Kitamura, J. Synchrotron Radiat. **19**, 388 (2012).

[27] As for the U $5f$ electrons, the orbital magnetic moment (M_{L}) is dominant and turns parallel to the external H direction, while the spin magnetic moment (M_{S}) is antiparallel to M_{L}. As for the Co $3d$ electrons, both the M_{S} and the M_{L} turn parallel to the H direction. As a result, the total magnetic moments ($M_{\mathrm{S}} + M_{\mathrm{L}}$) for both the U $5f$ and Co $3d$ electrons are parallel to the H direction, as discussed in the previous XMCD study [25].

[28] M. Kučera, J. Kuneš, A. Kolomiets, M. Diviš, A. V. Andreev, V. Sechovský, J.-P. Kappler, and A. Rogalev, Phys. Rev. B **66**, 144405 (2002).

[29] T. Combier, A. Palacio-Morales, J.-P. Sanchez, F. Wilhelm, A. Pourret, J.-P. Brison, D. Aoki, and A. Rogalev, J. Phys. Soc. Jpn. **86**, 024712 (2017).

[30] There are differences between the XMCD spectra obtained by the two XMCD experiments at the U $M_{4,5}$ edges. Therefore, the differences cause a relatively large error in the estimation of the integral value at the U $N_{4,5}$ edges, as denoted by a gray wide bar.

[31] The peculiar shape of the XMCD spectrum at the Co L_2 edge is always observed under the experimental conditions we have measured, namely, both in the PM state and the field-induced FM state, as reported in Ref. [25].

[32] C. T. Chen, Y. U. Idzerda, H.-J. Lin, N. V. Smith, G. Meigs, E. Chaban, G. H. Ho, E. Pellegrin, and F. Sette, Phys. Rev. Lett. **75**, 152 (1995).

[33] F. Wilhelm, J. P. Sanchez, J.-P. Brison, D. Aoki, A. B. Shick, and A. Rogalev, Phys. Rev. B **95**, 235147 (2017).

[34] The H dependence of the XMCD intensity was measured along a loop pathway ($H = 7 \rightarrow -7 \rightarrow 7$ T). Since the XMCD data are averaged for $\pm H$ in order to improve the precision of the data, the hysteresis behavior was erased.

[35] V. Sechovsky, L. Havela, F. de Boer, J. Franse, P. Veenhuizen, J. Sebek, J. Stehno, and A. Andreev, Physica B+C **142**, 283 (1986).

[36] R. J. Papoular and A. Delapalme, Phys. Rev. Lett. **72**, 1486 (1994).

Correction: The previously published Figure 6 contained an error in the symbol key and has been replaced.